Study of the Reaction $ClO + CH_3O_2 \rightarrow$ Products at 300 K

F. G. Simon, J. P. Burrows,* W. Schneider, G. K. Moortgat,* and P. J. Crutzen

Air Chemistry Department, Max-Planck-Institut für Chemie, Saarstrasse 23, D-6500 Mainz, FRG
(Received: January 12, 1989; In Final Form: June 9, 1989)

The first experimental study of the reaction $ClO + CH_3O_2 \rightarrow$ products (1) is reported. The rate coefficient k_1 and the product distributions were investigated in the modulated photolysis of $Cl_2/CH_4/Cl_2O/O_2$ mixtures. Reactants and products have been monitored by using UV-vis and Fourier-transform infrared gas-phase absorption spectroscopies. The value of k_1 was found to be equal to $(3.1 \pm 1.7) \times 10^{-12}$ cm^3 molecule^{-1} s^{-1} at 300 K and 240 Torr total pressure. The product channel forming ClOO and CH_3O appears to be the dominant pathway at 300 K. The subsequent oxidation of CH_3O to CH_2O and its partial photolysis into H and HCO leads to enhanced production of odd hydrogen (OH, HO_2) radicals. Consequently, high concentrations of OH radicals can build up, leading to an additional source of active chlorine via the reaction $HCl + OH \rightarrow Cl + H_2O$, which destroys ozone by catalytic reactions. This strongly suggests that reaction 1 can play a substantial role in the photochemical processes that take place under stratospheric "ozone hole" conditions.

Introduction

The discovery of the so-called "ozone hole", the increasingly precipitous loss of much of the ozone in the stratosphere below 22 km during the months of September to November over Antarctica,[1,2] has spurred much scientific research into the possible meteorological or chemical processes that can explain this unexpected phenomenon.

After only a few years of highly successful and innovative research efforts, it is now clear, that under the prevailing meteorological conditions in the Antarctic stratosperic spring, the loss of ozone is due to photochemical destruction by reactions involving ClO_x compounds derived mainly from the industrial chlorofluorocarbon gases $CFCl_3$ and CF_2Cl_2.[3-5] In brief the following steps appear now to constitute the main mechanism for the rapid ozone depletion over Antarctica:

1. The extremely low temperatures that occur during the winter and early spring months lead to the formation of two kinds of ice particles, polar stratospheric clouds (PSC) type I, consisting mostly of nitric acid trihydrate (NAT) and type II-PSC particles consisting mainly of water ice (ICE). The NAT particles occur more frequently than ICE particles, because they can form at temperatures around 195 K, almost 10 K higher than that required for ICE particle formation.[6-11]

2. During the polar night NO_x (NO and NO_2) is converted to N_2O_5, which reacts with the particles and becomes incorporated as HNO_3 in the PSC's. Due to this process the stratosphere loses much of its gaseous NO_x.[12,13]

3. HCl can likewise be incorporated in both the NAT and ICE particles, but because of a high HCl/HNO_3 ratio, efficient heterogeneous reactions may take place particularly on the NAT particles, converting HCl and $ClONO_2$ into gaseous $ClNO_2$ and Cl_2[14-17]

$$HCl + ClONO_2 \rightarrow Cl_2 + HNO_3 \text{ (NAT)}$$

$$HCl + N_2O_5 \rightarrow ClNO_2 + HNO_3 \text{ (NAT)}$$

However, $ClONO_2$ may also react on the surface of the particles with H_2O, releasing HOCl into the gas phase and depositing HNO_3 onto the particles.[7] An equivalent set of reactions, leading to the release of Cl_2 into the gas phase, is[18]

$$ClONO_2 + H_2O \text{ (ICE, NAT)} \rightarrow HOCl + HNO_3 \text{ (NAT, ICE)}$$

$$HCl \text{ (ICE, NAT)} + HOCl \rightarrow Cl_2 + H_2O \text{ (NAT, ICE)}$$

4. At the end of the polar winter, as soon as solar radiation impinges again on the lower stratosphere, Cl_2, $ClNO_2$, and HOCl, are rapidly photolyzed yielding Cl and starting a catalytic ozone destruction cycle,[19] which is particularly effective in the ozone hole region of the lower stratosphere

$$(Cl + O_3 \rightarrow ClO + O_2) \times 2$$

$$ClO + ClO + M \rightarrow Cl_2O_2 + M$$

$$Cl_2O_2 + h\nu \rightarrow Cl + ClOO$$

$$ClOO + M \rightarrow Cl + O_2 + M$$

Net: $$2O_3 + h\nu \rightarrow 3O_2$$

An additional mechanism by which ClO_x catalyzed ozone destruction can be activated was suggested by Crutzen and Arnold[7] who proposed that the loss of NO_2 and HNO_3 from the lower stratosphere would facilitate the formation of OH and HO_2 radicals leading to the conversion of HCl to Cl

$$HCl + OH \rightarrow Cl + H_2O$$

This production of Cl leads to the removal of ozones by the cycle described above and, in addition, via[20]

$$OH + O_3 \rightarrow HO_2 + O_2$$

$$Cl + O_3 \rightarrow ClO + O_2$$

$$ClO + HO_2 \rightarrow HOCl + O_2$$

$$HOCl + h\nu \rightarrow Cl + OH$$

Net: $$2O_3 + h\nu \rightarrow 3O_2$$

According to Crutzen and Arnold[7] the initial buildup of the HO_x

(1) Farman, J. D.; Gardner, B. G.; Shanklin, J. D. *Nature* **1985**, *315*, 207.
(2) Chubachi, S.; Kajiwara, R. *Geophys. Res. Lett.* **1986**, *13*, 1197.
(3) Solomon, S.; Mount, G. H.; Sanders, R. W.; Schmeltekopf, A. L. *Geophys. Res. Lett.* **1987**, *92*, 8329.
(4) Anderson, J. G.; Brune, W. H.; Profitt, M. J.; Starr, W.; Chan, K. R. Polar Ozone Workshop 1988, Snowmass, CO, NASA Conf. Publ. 10014.
(5) DeZafra, R. L.; Jaramillo, M.; Parrish, A.; Solomon, P.; Connor, B.; Barnett, J. *Nature* **1987**, *328*, 408.
(6) Toon, O. B.; Hamill, R.; Turco, R. P.; Pinto, J. *Geophys. Res. Lett.* **1986**, *13*, 1284.
(7) Crutzen, P. J.; Arnold, F. *Nature* **1986**, *324*, 651.
(8) Hanson, D.; Mauersberger, K. *J. Phys. Chem.* **1988**, *92*, 6167.
(9) Hanson, D.; Mauersberger, K. *Geophys. Res. Lett.* **1988**, *15*, 855.
(10) Poole, L. R.; McCormick, P. *Geophys. Res. Lett.* **1988**, *15*, 21.
(11) Hanson, D.; Mauersberger, K., submitted for publication in *Geophys. Res. Lett.*
(12) Keys, J. G.; Johnston, P. V. *Geophys. Res. Lett.* **1986**, *13*, 1260.
(13) Shibasaki, K.; Iwagami, N.; Ogawa, T. *Geophys. Res. Lett.* **1986**, *13*, 1268.
(14) Molina, M. J.; Tso, T. L.; Molina, L. T.; Wang, F. C. Y. *Science* **1987**, *238*, 1253.
(15) Tolbert, M. J.; Rossi, M. J.; Malhotra, R.; Golden, D. M. *Science* **1987**, *238*, 1258.
(16) Tolbert, M. J.; Rossi, M. J.; Golden, D. M. *Science* **1988**, *240*, 1018.
(17) Leu, M. T. *Geophys. Res. Lett.* **1988**, *15*, 851.
(18) Crutzen, P. J.; Brühl, C.; Schmailzl, U.; Arnold, F. *Aerosols and Climate*; McCormick, M. P., Hobbs, P. V., Eds.; A. Deepak Publ.: Hampton, VA, 1988.
(19) Hayman, G. D.; Cox, R. A. *Nature* **1988**, *332*, 796.
(20) Solomon, S.; Garcia, R. R.; Rowland, F. S.; Wuebbles, D. J. *Nature* **1986**, *321*, 755.

0022-3654/89/2093-7807$01.50/0

TABLE I: Absorption Cross Sections σ, in cm^2 molecule^{-1}, Used in This Work

molecule	wavelength, nm 240	260	292	370	ref
Cl_2		1.38×10^{-21}	6.95×10^{-20}	8.30×10^{-21}	23
Cl_2O	9.82×10^{-19}	1.83×10^{-18}	9.40×10^{-19}	5.58×10^{-21}	24, 25
ClO[a]	2.22×10^{-18}	5.04×10^{-18}	3.40×10^{-18}	–	25
OClO[b]		2.31×10^{-19}	1.14×10^{-18}	3.73×10^{-18}	26
CH_3O_2	4.58×10^{-18}	3.16×10^{-18}	6.35×10^{-19}	–	27

[a] Resolution 0.3 nm. [b] Resolution 0.25 nm.

radicals (HO_2 and OH) would be enhanced by a chain reaction involving the methane oxidation cycle. In this paper we will considerably strengthen this proposal by reporting the results of the first experimental study on the role of ClO in the CH_4 oxidation chain via the reaction

$$ClO + CH_3O_2 \rightarrow \text{products} \quad (1)$$

In order to examine this mechanism, both the rate coefficient and the product distribution of this reaction have been investigated at 300 K.

Experimental Section

All experiments were performed in a modulated photolysis "double multipath" absorption apparatus, which is described in detail elsewhere.[21] It consists of a 44.2-L quartz photochemical chamber, surrounded by six fluorescent "sun lamps" (Philips TL40/12, λ_{max} = 310 nm). The lamps can be switched on and off at frequencies between 2.5 kHz and 0.02 Hz and the ratio of "light on" time to "light off" time can be varied from 0.1 to 9. Reactants, products, and transient species were monitored by long path absorption using either a Fourier-transform-infrared (FTIR) spectrometer (BOMEM DA03, optical length = 43.2 m) or a UV absorption spectrometer (B&M 50, optical length = 9.8 m) with a 600 lines/mm grating (dispersion 3.2 nm/mm) blazed at 200 nm. The UV light beam from a 200-W deuterium lamp (Heraeus) was detected by either a photomultiplier (R106UH Hamamatsu) or a 25 mm 1024 pixel silicon diode array detector (EG&G Model 1461 + 1412).

The bulk flows of Cl_2, Cl_2O, CH_4, and O_2 were set by using calibrated flow controllers (Tylan FC 260, FC 280), prior to their entry into the cell. The residence time of the gases in the cell was about 30 s and the total pressure 230–240 Torr. Typically the initial concentrations of reactants were $Cl_2 = (3\text{–}4) \times 10^{15}$, $Cl_2O = (0\text{–}1.5) \times 10^{14}$, $CH_4 = (0\text{–}1.0) \times 10^{17}$, $O_2 = (7\text{–}8) \times 10^{18}$ molecules cm^{-3}.

Cl_2O was prepared by flowing chlorine (ca. 1% in nitrogen) through a column packed with yellow mercuric oxide.[22] Chlorine (ca. 1% in nitrogen grade 3.8, Linde), methane (grade 3.5, Linde), and oxygen (grade 4.5, Linde) were used without further purification. The initial concentrations of Cl_2 and Cl_2O were determined from absorption measurements in the UV region at 370 and 260 nm, respectively. The modulated absorptions at 240 and 292 nm were used to investigate the ClO and CH_3O_2 behavior. The absorption cross sections of Cl_2, Cl_2O, OClO, ClO, and CH_3O_2 are listed in Table I at the different wavelengths used.

Results

(*a*) *Photolysis of the Chemical System $Cl_2/Cl_2O/CH_4/O_2$.* The following reactions take place in the photolysis of $Cl_2/Cl_2O/O_2$ mixtures:

$$Cl_2 + h\nu \rightarrow Cl + Cl \quad (2)$$

$$Cl_2O + h\nu \rightarrow ClO + Cl \quad (3)$$

$$Cl + Cl_2O \rightarrow Cl_2 + ClO \quad (4)$$

$$ClO + ClO \rightarrow Cl_2 + O_2 \quad (5a)$$

$$ClO + ClO \rightarrow Cl + ClOO \quad (5b)$$

$$ClO + ClO \rightarrow Cl + OClO \quad (5c)$$

$$ClO + ClO + M \leftrightarrow Cl_2O_2 + M \quad (5d)$$

$$ClOO + M \rightarrow Cl + O_2 + M \quad (6)$$

This reactive system has been studied in detail by Cox et al.[19,28] The ClO radical is mainly produced by the sequence of reactions 2 and 4. The contribution to the production of ClO by the photolysis of Cl_2O is about 5% of that due to the photolysis of Cl_2 followed by reaction 4 under the conditions used here. The major loss process of ClO is the slow self-reaction ($k_{5a+5b+5c} = 2.36 \times 10^{-14}$ cm^3 molecule^{-1} s^{-1}, $K_{5d} = 5.2 \times 10^{-15}$ cm^3 molecule^{-1}),[19,28] which has several product channels. Due to the regeneration of the chlorine atoms in channels 5b and 5c, ClO is also formed during the dark phase of the modulated photolysis cycle.

CH_3O_2 radicals are produced in the photolysis of $Cl_2/CH_4/O_2$ mixtures by the reactions

$$Cl_2 + h\nu \rightarrow Cl + Cl \quad (2)$$

$$Cl + CH_4 \rightarrow CH_3 + HCl \quad (7)$$

$$CH_3 + O_2 + M \rightarrow CH_3O_2 + M \quad (8)$$

and subsequently react via the following reactions:

$$CH_3O_2 + CH_3O_2 \rightarrow CH_3O + CH_3O + O_2 \quad (9a)$$

$$CH_3O_2 + CH_3O_2 \rightarrow CH_3OH + CH_2O + O_2 \quad (9b)$$

$$CH_3O_2 + CH_3O_2 \rightarrow CH_3O_2CH_3 + O_2 \quad (9c)$$

$$CH_3O + O_2 \rightarrow CH_2O + HO_2 \quad (10)$$

$$CH_3O_2 + HO_2 \rightarrow CH_3OOH + O_2 \quad (11a)$$

$$CH_3O_2 + HO_2 \rightarrow CH_2O + H_2O + O_2 \quad (11b)$$

The CH_3O_2 radicals are formed from the system by the self-reaction (9) and the cross disproportionation reaction (11) with HO_2 radicals. HO_2 radicals and CH_2O are produced by reaction 10 between CH_3O and O_2. Since two CH_3O radicals are oxidized to HO_2 and CH_2O, and because reaction 11 is fast ($k_{11} = 6.0 \times 10^{-12}$ cm^3 molecule^{-1} s^{-1}), the overall rate coefficient for loss of CH_3O_2 in $Cl_2/CH_4/O_2$ mixtures, $k_{removal}$, is given by ($2k_{9a} + k_{9b} + k_{9c}$). The rate constant for the self-reaction $k_9 = (k_{9a} + k_{9b} + k_{9c})$ has recently been investigated in this laboratory in the same apparatus and a value for k_9 of $(3.58 \pm 0.24) \times 10^{-13}$ cm^3 molecule^{-1} s^{-1} at 298 K was determined.[27]

(21) Moortgat, G. K.; Cox, R. A.; Schuster, G.; Burrows, J. P.; Tyndall, G. S. *J. Chem. Soc., Faraday Trans. 2*, in press.
(22) Gay-Lussac, J. L. *Ann. Chim. Phys.* **1842**, *43*, 153.
(23) Schneider, W.; Moortgat, G. K., paper in preparation.
(24) Lin, C. L. *J. Chem. Eng. Data* **1976**, *21*, 411.
(25) Simon, F. G. Ph.D. Thesis, University Mainz, 1989.
(26) Wahner, A.; Tyndall, G. S.; Ravishankara, A. R. *J. Phys. Chem.* **1987**, *91*, 2734.
(27) Simon, F. G.; Schneider, W.; Moortgat, G. K., submitted for publication in *Int. J. Chem. Kinet.*
(28) Burrows, J. P.; Cox, R. A. *J. Chem. Soc., Faraday Trans. 1* **1981**, *77*, 2465.

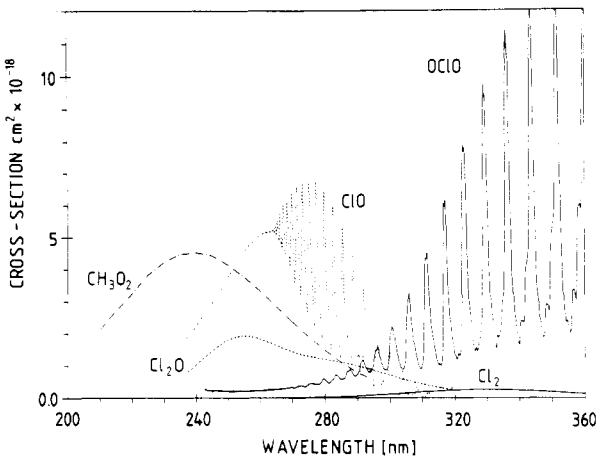

Figure 1. Absorption spectra of CH_3O_2 (–·–) from ref 27, ClO (···) from ref 25, OClO (〰) from ref 26, Cl_2 (—) from ref 23, and Cl_2O (- - -) from ref 25.

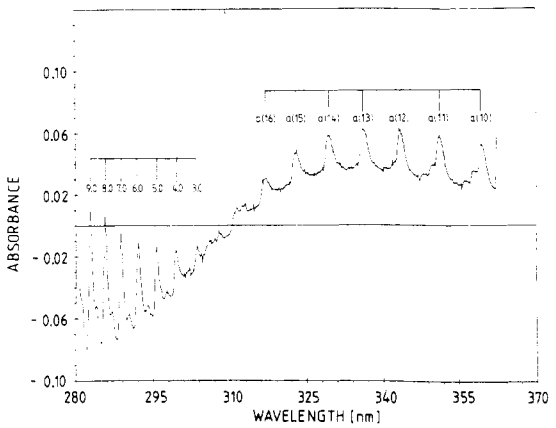

Figure 2. ClO (280–310 nm) and OClO (300–360 nm) product absorption in the photolysis of $Cl_2/Cl_2O/O_2$ mixtures observed by the diode array camera.

When mixtures of Cl_2, Cl_2O, CH_4, and O_2 are photolyzed, both ClO and CH_3O_2 radicals are generated via reactions 3 and 4 and reactions 7 and 8, respectively. As the rate coefficients for reactions 4 and 7 differ by 3 orders of magnitude ($k_4 = 9.8 \times 10^{-11}$ cm^3 molecule^{-1} s^{-1} and $k_7 = 1.0 \times 10^{-13}$ cm^3 molecule^{-1} s^{-1}), the concentration ratio, $[CH_4]/[Cl_2O]$, required for equal ClO and CH_3O_2 production rates is approximately 1000.

In order to study the kinetics of reaction 1

$$ClO + CH_3O_2 \rightarrow \text{products} \qquad (1)$$

the ClO and CH_3O_2 behavior in photolyzed $Cl_2/Cl_2O/CH_4/O_2$ mixtures was investigated by UV–vis absorption spectroscopy. In the UV, ClO has a banded spectrum in the region between 270 and 310 nm,[25,29–31] whereas CH_3O_2 has a broad band absorption feature between 200 and 280 nm, with a maximum at 240 nm.[27] The absorption spectra are displayed in Figure 1. In the modulated photolysis of $Cl_2/Cl_2O/CH_4/O_2$ mixtures, the behavior of ClO was determined from optical density measurements at 292.2 nm (6,0 band). Optical density changes were also monitored at 240 nm, where both ClO and CH_3O_2 absorb. At both these wavelengths, additional changes in absorption due to the reactant gases Cl_2 and Cl_2O, whose spectra are also shown in Figure 1, must be taken into account during the kinetic analysis (see also Table I). The detection limit for ClO was 3×10^{11} molecules cm^{-3} at 292 nm.

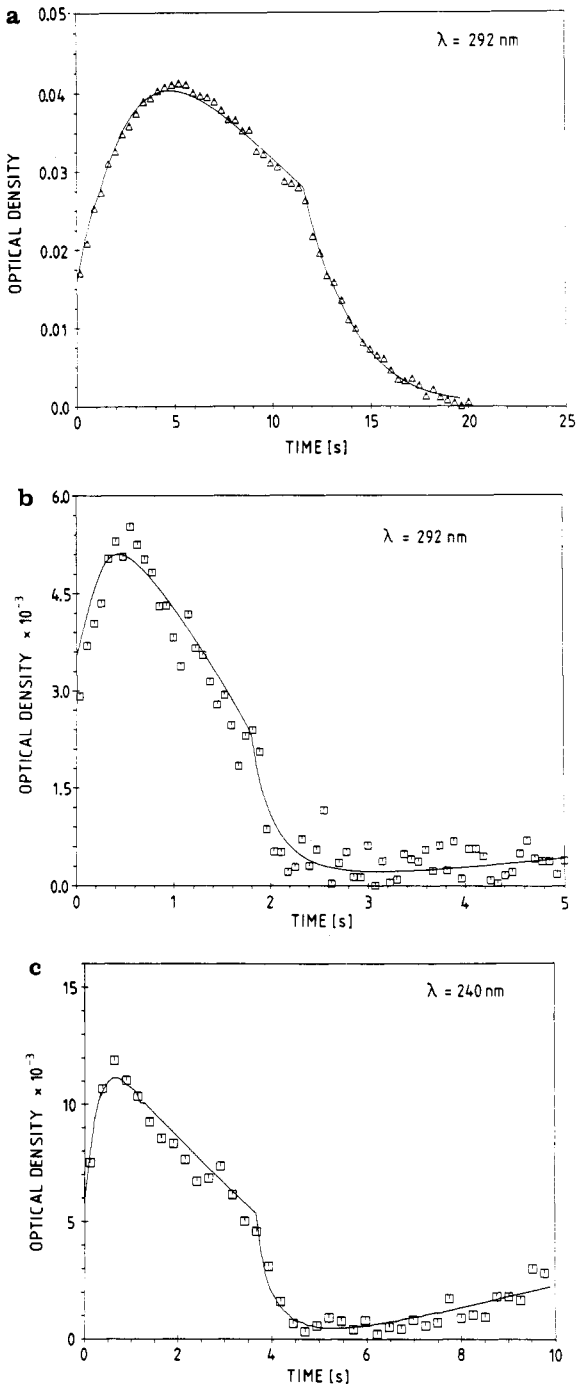

Figure 3. Time-dependent absorption observed during the modulated photolysis of $Cl_2/Cl_2O/CH_4/O_2$ mixtures. The dark phase of the periods starts after 11.7 (a), 1.8 (b), and 3.7 s (c), respectively. (a) $CH_4 = 0$ molecule cm^{-3}, total period 30 s, $\lambda = 292$ nm. (b) $CH_4 = 1.36 \times 10^{17}$ molecules cm^{-3}, total period 10 s, $\lambda = 292$ nm. (c) $CH_4 = 1.36 \times 10^{17}$ molecules cm^{-3}, total period 20 s, $\lambda = 240$ nm.

In the first set of experiments the photolysis of $Cl_2/Cl_2O/O_2$ mixtures was studied without the addition of CH_4. Figure 2 shows the product absorption observed by the diode array camera in a 82-nm frame between 280 and 362 nm: here both ClO and OClO are detected simultaneously. The negative background absorption in the range 280–310 nm, on which the sharp ClO bands are superimposed, is due to the loss of Cl_2O by photolysis. Both OClO and Cl_2 are products of the disproportionation of ClO radicals[28] and show positive absorption features at wavelengths longer than ca. 310 nm. Cl_2 is also produced by reaction 4. The observed ClO absorption bands agree with the measurements of Mandelman and Nicholls.[30] A more detailed spectrum and a study of this system are to be published elsewhere.[31] The observed OClO absorption spectrum is in good agreement with the recent data

(29) Watson, R. T. *J. Phys. Chem. Ref. Data* **1977**, *6*, 871.
(30) Mandelman, N.; Nicholls, R. W. *J. Quant. Spectrosc. Radiat. Transfer* **1977**, *17*, 483.
(31) Simon, F. G.; Schneider, W.; Moortgat, G. K.; Burrows, J. P. submitted for publication in *J. Photochem. Photobiol. A.*

TABLE II: Reaction Mechanism Involved in the $Cl_2/Cl_2O/CH_4/O_2$ Photolysis

reaction		rate constant, cm^3 molecule^{-1} s^{-1}	ref
2	$Cl_2 + h\nu \rightarrow Cl + Cl$	5.8×10^{-4} [a]	this work
3	$Cl_2O + h\nu \rightarrow ClO + Cl$	1.3×10^{-3} [a]	this work
4	$Cl + Cl_2O \rightarrow Cl_2 + ClO$	9.8×10^{-11}	33
7	$Cl + CH_4 \rightarrow CH_3 + HCl$	1.0×10^{-13}	33
8	$CH_3 + O_2 + M \rightarrow CH_3O_2 + M$	4.5×10^{-31} [b]	33
5a	$ClO + ClO \rightarrow Cl_2 + O_2$	8.2×10^{-15}	28
5b	$\rightarrow Cl + ClOO$	7.4×10^{-15}	28
5c	$\rightarrow OClO + Cl$	8.0×10^{-15}	28
5d	$ClO + ClO + M \Leftrightarrow Cl_2O_2 + M$	5.2×10^{-15} [c]	19
9a	$CH_3O_2 + CH_3O_2 \rightarrow CH_3O + CH_3O + O_2$	1.1×10^{-13}	27
9b	$\rightarrow CH_2O + CH_3OH + O_2$	2.2×10^{-13}	27
9c	$\rightarrow CH_3O_2CH_3 + O_2$	2.9×10^{-14}	27
1	$ClO + CH_3O_2 \rightarrow CH_3O + ClOO$	3.1×10^{-12}	this work
6	$ClOO + M \rightarrow Cl + O_2 + M$	3.3×10^{-13}	28
10	$CH_3O + O_2 \rightarrow CH_2O + HO_2$	1.5×10^{-15}	33
11a	$CH_3O_2 + HO_2 \rightarrow CH_3OOH + O_2$	3.0×10^{-12}	33, 34
11b	$\rightarrow CH_2O + H_2O + O_2$	3.0×10^{-12}	33, 34
12	$ClO + HO_2 \rightarrow HOCl + O_2$	5.4×10^{-12}	28
13	$HO_2 + HO_2 \rightarrow H_2O_2 + O_2$	1.7×10^{-12}	33
14	$HO_2 + CH_2O \rightarrow HOCH_2O_2$	6.6×10^{-14}	35
−14	$HOCH_2O_2 \rightarrow HO_2 + CH_2O$	100[a]	35
15	$HOCH_2O_2 + HO_2 \rightarrow HCOOH + H_2O + O_2$	4.8×10^{-12}	35
16	$2HOCH_2O_2 \rightarrow 2HOCH_2O + O_2$	5.2×10^{-12}	35
17	$HOCH_2O + O_2 \rightarrow HCOOH + HO_2$	3.5×10^{-14}	35
18	$Cl + CH_3OH \rightarrow CH_2OH + HCl$	6.3×10^{-11}	33
19	$CH_2OH + O_2 \rightarrow CH_2O + HO_2$	9.6×10^{-12}	33
20	$Cl + CH_2O \rightarrow HCO + HCl$	7.3×10^{-11}	33
21	$HCO + O_2 \rightarrow HO_2 + CO$	5.5×10^{-12}	33
22	$Cl + ClOO \rightarrow Cl_2 + O_2$	9.8×10^{-11}	28
23	$Cl + OClO \rightarrow ClO + ClO$	5.9×10^{-11}	28
24	$OClO + h\nu \rightarrow ClO + O$	1.0×10^{-2} [a]	this work
25	$O + O_2 + M \rightarrow O_3 + M$	6.0×10^{-34} [b]	33

[a] Unit s^{-1}. [b] Unit cm^6 molecule^{-2} s^{-1}. [c] Equilibrium constant unit cm^3 molecule^{-1}.

of Wahner et al.[26] The detection limit for OClO in our system is 1.0×10^{11} molecules cm^{-3} for the strongest absorption band.

The time-dependent behavior of the absorption at 292.2 nm, observed during the modulated photolysis of $Cl_2/Cl_2O/O_2$ mixtures, is shown in Figure 3a. After the lamps are switched on, the absorption rises until ClO reaches a steady-state concentration. This absorption then decreases due to the removal of Cl_2O by reactions 3 and 4. When the photolysis lamps are switched off, ClO absorption decreases because ClO is removed by reaction 5, which produces the stable products OClO, Cl_2, and O_2. Cl atoms are regenerated by reactions 5b and 5c and subsequently react via reaction 4 to produce ClO. Finally, during the last part of the period (not shown in Figure 3a) the absorption signal increases due to the flow-in of reactants, mainly Cl_2O.

Upon the addition of CH_4 to the $Cl_2/Cl_2O/O_2$ mixture, the observed absorption waveform changes drastically. Parts b and c of Figure 3 show the time dependence of the absorption in the modulated photolysis of a $Cl_2/Cl_2O/CH_4/O_2$ mixture at 292.2 and 240 nm, respectively. In this case a lower ClO steady-state absorption at 292.2 nm is obtained at a shorter time after the lamps are ignited. When the lamps are switched off, this absorption decays rapidly. At 240 nm (Figure 3c), where both ClO and CH_3O_2 absorb, the absorption trace is similar to that obtained at 292 nm (Figure 3b). These observations are best explained by postulating a fast bimolecular reaction between ClO and CH_3O_2, reaction 1.

(*b*) *Determination of* $k_{ClO+CH_3O_2}$. In order to obtain the rate constant for reaction 1, the time-dependent absorption data recorded at 240 and 292 nm were fitted to a chemical model. The computer program FACSIMILE[32] was used for this purpose and the value of k_1 was varied and its optimum value obtained by a least-squares fitting procedure.

TABLE III: Experimental Data[a]

concn of Cl_2O, 10^{14} cm^{-3}	concn of CH_4, 10^{17} cm^{-3}	$k_7[CH_4]/k_4[Cl_2O]$	$k_1 \times 10^{12}$, cm^3 molecule^{-1} s^{-1}
1.44	0.84	0.59	4.07
0.74	1.76	2.43	1.94
1.50	6.74	4.59	4.60
1.50	6.82	4.64	3.69
1.50	3.14	2.14	2.20
1.15	1.36	1.21	3.06
1.15	1.36	1.21	2.77
1.15	0.61	0.54	2.94
1.15	0.41	0.37	2.97
1.08	0.34	0.37	3.90
1.08	0.34	0.37	2.26
1.08	1.32	1.25	2.06
1.08	1.32	1.25	3.58
1.08	0.71	0.67	3.14
1.08	0.71	0.67	3.14

[a] All experiments were performed at 298 K and 240 ± 10 Torr total pressure.

The chemical reaction mechanism used to fit the absorption data is described in Table II. Flow into and out of the system was modeled assuming that the cell is well mixed, i.e. $k_{flowout} = 1/t_{res}$ and $k_{flowin} = k_{flowout}[X]$.

(32) Chance, E. M.; Curtis, A. R.; Jones, I. P.; Kirby, C. R. FACSIMILE Report AERE-R 8775, AERE Harwell 1977.

(33) Demore, W. B.; Molina, M. J.; Sander, S. P.; Golden, D. M.; Hampson, R. F.; Kurylo, M. J.; Howard, C. J.; Ravishankara, A. R. "Chemical Kinetics and Photochemical Data for use in Stratospheric Modeling"; Jet Propulsion Lab, CA, 1987, Publication No. 87-41.

(34) Jenkin, M. E.; Cox, R. A.; Hayman, G. D.; Whyte, L. J. *J. Chem. Soc., Faraday Trans. 2* **1988**, *84*, 913.

(35) (a) Veyret, B.; Lesclaux, R.; Rayez, M. T.; Rayez, J. C.; Cox, R. A.; Moortgat, G. K. *J. Phys. Chem.* **1989**, *93*, 2368. (b) Burrows, J. P.; Moortgat, G. K.; Tyndall, G. S.; Cox, R. A.; Jenkin, M. E.; Hayman, G. D.; Veyret, B. *J. Phys. Chem.* **1989**, *93*, 2375.

(36) Kafafi, S. A.; Martinez, R. I.; Herron, J. T. *Molecular Structure and Energetics*; VCH Publishers: Deerfield Beach, FL, 1987. A value of 188 kJ/mol is recommended by the authors for CH_2OO (planar dioxymethylene).

(37) Herron, J. T.; Martinez, R. I., private communication. The perpendicular state of CH_2OO, which is believed to be formed in this reaction, lies about 125 kJ/mol higher than the ground state (planar dioxymethylene).

(38) Benson, S. W. *Thermochemical Kinetics*; Wiley: New York, 1976.

TABLE IV: Possible Reaction Channels for CH_3O_2 and ClO

reaction channel		$\Delta H_R(298)$,[a] kJ/mol
1a	$CH_3O_2 + ClO \rightarrow ClOO + CH_3O$	-9.2 ± 13
1b	$\rightarrow OClO + CH_3O$	-7.1 ± 16
1c	$\rightarrow CH_2O + HCl + O_2$	-319.3 ± 8
1d	$\rightarrow CH_2OO + HOCl$	$+118.0 \pm 8$
1e	$\rightarrow CH_3O + Cl + O_2$	$+17.6 \pm 8$
1f	$\rightarrow CH_3Cl + O_3$	-57.4 ± 8
1g	$\rightarrow CH_3OCl + O_2$	-178 ± 8

[a] ΔH_R calculated with the ΔH_f from ref 33, except for CH_2OO (perpendicular dioxymethylene), ref 36 and 37, and for CH_3OCl, with additivity rules from ref 38.

The experimental conditions and the computer-fitted values for k_1 are summarized in Table III. The value of k_1 determined appears to be independent of the ratio of the rates of production of the two radicals CH_3O_2 and ClO, $k_7[CH_4]/k_4[Cl_2O]$, which was varied from 0.3 to 5. A mean value for k_1 of $(3.1 \pm 1.5) \times 10^{-12}$ cm^3 molecule^{-1} s^{-1} at 298 K and 240 Torr (error = 2 × standard deviation) was obtained. Computer fits of the absorption trace are superimposed on the experimental data points in Figure 3 (a, b, and c).

In order to estimate the error in the determination of k_1, the sensitivity of the fitted k_1 to changes in the parameters used in that fit (i.e. rate constants and absorption cross sections) was investigated. The following results were obtained:

(i) Reducing the chemical mechanism to reactions 1, 2, and 4–12 had little effect on the fitting, showing that k_1 was determined predominantly by this simplified reaction scheme.

(ii) Due to the presence of 200 Torr O_2, the decomposition of ClOO, reaction 6, and the reactions of CH_3 and CH_3O with O_2 (8 and 10) occur rapidly. Consequently any uncertainty in the rate coefficients k_6, k_8, and k_{10} does not contribute to the uncertainty in k_1. The flux of reaction 5d compared to the other three reaction pathways (5a–c) is less than 5% at 300 K; therefore the equilibrium reaction (5d) does not have an important effect on the value of k_1 determined.

(iii) An increase of the ClO cross section at 292 nm of 25% produces an increase of 9% in k_1; a decrease in the absorption cross section of ClO at 240 nm by 15% resulted in a change of k_1 of 8%.

(iv) A decrease in the rate coefficient for reaction 5 by a factor of 2 yielded a fitted k_1 reduced by 7%.

(v) An increase of the photolysis rate k_2 by 25% leads to a decrease in k_1 of 20%.

(vi) Increasing k_9 by 25% caused a variation of k_1 of approximately 11%.

(vii) The role played by the product of the reaction between ClO and CH_3O_2 in this system is not trivial. The reaction product channels are listed in Table IV and discussed in the following section. Simulations showed that the flux of molecules reacting through the reaction between ClO and HO_2 is approximately 0.8 of that through the reaction between ClO and CH_3O_2, assuming that pathway 1a dominates. This implies that if the reaction proceeded through pathway 1c, then k_1 would be approximately 80% larger. A further simulation showed that in the absence of a rapid reaction between ClO and CH_3O_2, the production of HO_2 via the disproportionation of CH_3O_2 requires a rate of ClO removal approximately 7.5 times slower than that required to explain the observed ClO behavior.

From observations i–vi, it can be seen that the uncertainty in the determination of the value of k_1 arises from the uncertainty in the Cl_2 photolysis rate measured in this work, and the uncertainties in the literature values for reactions 5 and 9, which have both been subject to recent investigations in this laboratory.[27,31] Combining the error estimates above with the experimental error obtained leads to a final value $k_1 = (3.1 \pm 1.7) \times 10^{-12}$ cm^3 molecule^{-1} s^{-1}. This determination assumes that the value of k_{ClO+HO_2} taken from the literature is correct. As can be seen in (vii) a change in this rate coefficient would affect the value of k_1.

(c) *$ClO + CH_3O_2$ Reaction Mechanism.* The products of reaction 1 were studied by investigation of the infrared and UV–vis absorptions. Several possible pathways are summarized in Table IV; also included are the reaction enthalpies for the various reactions.

Inspection of these values shows that channels 1d and 1e can be ignored because of their endothermicity. If channel 1f occurs, then the formation of ozone is predicted. No evidence for the formation of O_3 from the absorption at 254 nm or from the infrared was observed. Channel 1f is therefore not considered to be important. The exothermic channel 1g produces CH_3OCl in analogy to the $ClO + HO_2 \rightarrow HOCl + O_2$ reaction. Careful analysis of our infrared spectra did not reveal any evidence for a compound having an O–Cl vibration; however, it may absorb weakly.

If reaction channel 1b is an important pathway, an enhanced production of OClO should be observable at wavelengths above 300 nm in the photolysis of mixtures of Cl_2, Cl_2O, CH_4, and O_2 as compared with Cl_2, Cl_2O, and O_2 mixtures. No detectable amounts of OClO were observed in the photolysis of $Cl_2/Cl_2O/CH_4/O_2$ mixtures and an upper limit for the branching ratio $k_{1b}/k_1 < 0.05$ was estimated by computer simulations.

Instead, significant amounts of CH_2O were observed from its characteristic banded UV absorption spectrum[39] in the wavelength range 280–360 nm. Both of the two remaining channels, 1a and 1c, lead to the production of CH_2O. Reaction 1c produces CH_2O directly, whereas reaction 1a generates CH_3O which reacts with O_2 to form CH_2O and HO_2

$$CH_3O + O_2 \rightarrow CH_2O + HO_2 \quad (10)$$

The reactions of the products HO_2 and CH_2O have been used in this study to distinguish between the two reaction paths. HO_2 radicals are removed from the system by the following reactions, some of which lead to HCOOH formation:[35]

$$CH_3O_2 + HO_2 \rightarrow CH_3OOH + O_2 \quad (11a)$$

$$CH_3O_2 + HO_2 \rightarrow CH_2O + H_2O + O_2 \quad (11b)$$

$$HO_2 + ClO \rightarrow HOCl + O_2 \quad (12)$$

$$HO_2 + HO_2 \rightarrow H_2O_2 + O_2 \quad (13)$$

$$HO_2 + CH_2O \leftrightarrow HOCH_2O_2 \quad (14)$$

$$HOCH_2O_2 + HO_2 \rightarrow HCOOH + H_2O + O_2 \quad (15)$$

$$2HOCH_2O_2 \rightarrow 2HOCH_2O + O_2 \quad (16)$$

$$HOCH_2O + O_2 \rightarrow HCOOH + HO_2 \quad (17)$$

In a set of experiments the products obtained from the continuous photolysis ($285 < \lambda < 330$ nm) of flowing $Cl_2/CH_4/O_2$ mixtures were analyzed by long path FTIR spectroscopy. CH_2O, CH_3OH, HCl, and HCOOH were identified as the most important products formed in this system.

Simulation of the $Cl_2/Cl_2O/CH_4/O_2$ system indicated that the appearance of HCOOH is a sensitive test of the amount of production of CH_2O and HO_2 from reaction 10, especially as HCOOH absorbs strongly in a region free of other product or reactant interferences (1105 cm^{-1}). Photolyzed mixtures of Cl_2, CH_4, and O_2 (without Cl_2O) generate CH_3O and HO_2 via reactions 9a and 10. However, the majority of the HO_2 formed reacts with CH_3O_2 and only part of the HO_2 formed reacts with CH_2O via reaction 14, leading to the formation of HCOOH. Photolyzed mixtures of Cl_2, Cl_2O, CH_4, and O_2 product CH_3O via reaction 1a. An enhanced production of HO_2 and CH_2O and therefore HCOOH is anticipated as amounts of Cl_2O are added to mixtures of $Cl_2/CH_4/O_2$, provided channel 1a is dominant.

Figure 4 shows plots of the anticipated yield of HCOOH in the photolysis of Cl_2, Cl_2O, CH_4, and O_2 mixtures relative to the yield in the photolysis of Cl_2, CH_4, and O_2 mixtures as a function

(39) Moortgat, G. K.; Klippel, W.; Möbus, K. H.; Seiler, W.; Warneck, P. Final Report 1980, FAA-EE-80-47.

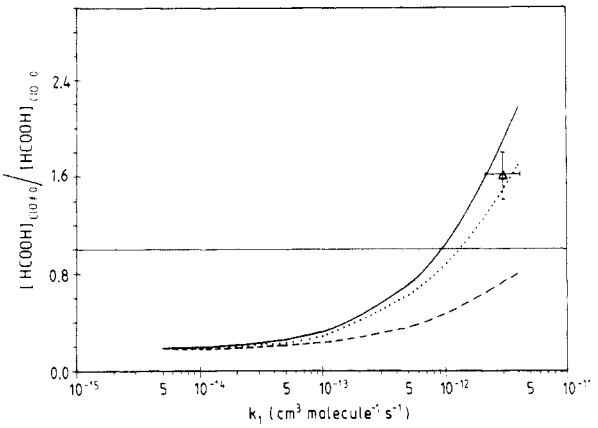

Figure 4. Calculated relative yield of HCOOH in the photolysis of $Cl_2/CH_4/O_2$ mixtures in the presence and absence of Cl_2O, as a function of reaction rate constant k_1. The experimental yield of HCOOH has been obtained by FTIR spectroscopy; curves are obtained by simulation using $k_{1a}/k_1 = 1$ (—) and $k_{1a}/k_1 = 0.8$ and $k_{1c}/k_1 = 0.2$ (···) and $k_{1c}/k_1 = 1$ (---).

of overall reaction rate k_1. Three curves are plotted: the solid curve represents the relative yield of HCOOH obtained from simulations where only pathway 1a occurs, i.e. $k_{1a}/k_1 = 1.0$; the dotted curve shows the relative HCOOH yield assuming $k_{1a}/k_1 = 0.7$ and $k_{1c}/k_1 = 0.3$; the dashed curve represents the relative HCOOH yield assuming only pathway 1c takes place, i.e. $k_{1c}/k_1 = 1.0$. Also plotted is the mean value of the relative experimental yield of HCOOH, which is the average of three experimental determinations. The yield of HCOOH is consistent with a branching ratio $k_{1a}/k_1 = 0.85 \pm 0.15$ for the experimentally obtained value of k_1.

Since HCl is a product of reaction pathway 1c, it would be possible to consider its yield as an indication of the occurrence of reaction 1c. HCl is produced predominantly by the reaction of Cl with CH_4. If reaction 1 proceeds via reaction 1a rather than reaction 1c, then Cl atoms are regenerated and a small increase in the production of HCl is anticipated than if (1c) alone was taking place. However simulation showed that the change in HCl yield obtained by substituting a model with only reaction pathway 1c with a model with only reaction pathway 1a was small. Therefore HCl measurements could not be used to determine whether channel 1a or 1c was dominant. On the basis of the above analysis channel 1c cannot be entirely ruled out. If reaction 1c occurs, it must proceed via an intermediate complex.

In conclusion, the simulations of the yield of HCOOH give an upper limit for the branching ratio $k_{1c}/k_1 < 0.3$ and a lower limit of $k_{1a}/k_1 > 0.7$ at 300 K.

Discussion

(*a*) *Kinetic Considerations.* The results obtained in this study show that ClO reacts rapidly with CH_3O_2 with a rate coefficient of $(3.1 \pm 1.7) \times 10^{-12}$ cm^3 molecule^{-1} s^{-1} at 300 K and a pressure of 240 Torr. The products of the reaction have also been studied and the reaction channel producing ClOO and CH_3O appears to be the dominant reaction pathway. This reaction product channel behavior may be considered by invoking an O-atom transfer mechanism.

Due to their important role in the chemistry of the atmosphere, many reactions of ClO and of peroxy radicals have been studied. The A factor and the Arrhenius activation temperature E/R for radical–radical O-atom transfer reactions of ClO and peroxy radicals are listed in Table V. It can be seen that most of these radical–radical reactions have small negative activation temperatures (E/R). This observation indicates that these O-atom transfer reactions proceed by first forming a complex which subsequently rearranges to form products, rather than the alternative of proceeding via a simple concerted atom transfer mechanism.

By comparison with the activation temperatures (listed in Table V) of the reaction of ClO with NO, ClO with OH, CH_3O_2 with NO, and HO_2 with NO, an activation temperature of approximately −200 K can be estimated, by analogy, for the reaction of ClO with CH_3O_2. This implies that at 190 K in the "ozone hole" the rate coefficient for the reaction between ClO and CH_3O_2 could be approximately $(4–5) \times 10^{-12}$ cm^3 molecule^{-1} s^{-1}.

TABLE V: O-Atom Transfer Reactions of ClO, HO_2, and CH_3O_2 Radical with Negative Activation Temperature

reaction	A factor,[33] cm^3 molecule^{-1} s^{-1}	E/R,[33] K
$ClO + O \rightarrow Cl + O_2$	3.0×10^{-11}	−(70 ± 70)
$ClO + NO \rightarrow Cl + NO_2$	6.4×10^{-12}	−(290 ± 100)
$ClO + OH \rightarrow Cl + HO_2$	1.1×10^{-11}	−(120 ± 150)
$HO_2 + NO \rightarrow OH + NO_2$	3.7×10^{-12}	−(240 ± 80)
$CH_3O_2 + NO \rightarrow CH_3O + NO_2$	4.2×10^{-12}	−(180 ± 180)

(*b*) *Stratospheric Implications of a Rapid ClO + CH_3O_2 Reaction.* The occurrence of a reasonably rapid reaction (1a) has a substantial influence in establishing large HO_x radical concentrations in the lower stratosphere under conditions in which both NO_x and HNO_3 are removed by uptake in stratospheric particles. Under these conditions, the catalytic cycles, which are effective at reducing HO_x concentrations

$$OH + NO_2 + M \rightarrow HNO_3 + M$$

$$OH + HNO_3 \rightarrow H_2O + NO_3$$

$$NO_3 + h\nu \rightarrow NO_2 + O$$

Net: $$2OH + h\nu \rightarrow H_2O + O$$

and

$$HO_2 + NO_2 + M \rightarrow HNO_4 + M$$

$$OH + HNO_4 \rightarrow H_2O + NO_2 + O_2$$

Net: $$OH + HO_2 \rightarrow H_2O + O_2$$

no longer take place.

Due to the absence of NO_x and the presence of elevated ClO concentrations, which may also result from heterogeneous reactions of HCl with $ClONO_2$, N_2O_5, and HOCl on the particles, the methane oxidation cycle will proceed via

$$CH_4 + OH + O_2 \rightarrow CH_3O_2 + H_2O$$

$$CH_3O_2 + ClO \rightarrow CH_3O + ClOO$$

$$ClOO + M \rightarrow Cl + O_2 + M$$

$$Cl + O_3 \rightarrow ClO + O_2$$

$$CH_3O + O_2 \rightarrow CH_2O + HO_2$$

Net: $$CH_4 + OH + O_3 \rightarrow CH_2O + H_2O + HO_2$$

This cycle implies no net loss of HO_x radicals. However, in the atmosphere CH_2O is photolyzed forming in part H and HCO (the product yield for this channel is approximately 0.3, the other channel gives H_2 + CO), which both produce HO_2

$$CH_2O + h\nu \rightarrow H + CHO$$

$$H + O_2 + M \rightarrow HO_2 + M$$

$$HCO + O_2 \rightarrow CO + HO_2$$

This implies that for each reaction of OH with CH_4 initially there will be a net gain of about $0.6HO_x$ (OH and HO_2) radicals. Some of the OH required to start the chain may be provided by the photolysis of HOCl. However, even if this were not the case, the chain would start with the reactions of CH_4 with Cl atoms, resulting from the photolysis of Cl_2O_2, which is certainly formed in the stratosphere via reaction 5d, as high concentrations of ClO have been measured under "ozone hole" conditions.[40] This leads to an active participation of OH and HO_2 radicals in the ClO_x

(40) Anderson, J. G.; Brune, W. H.; Profitt, M. H. *J. Geophys. Res.*, in press.

and O_3 chemistry of the polar stratosphere. The accumulation of HO_x radicals continues until the reaction

$$CH_3O_2 + HO_2 \rightarrow CH_3OOH + O_2$$
$$\rightarrow CH_2O + H_2O + O_2$$

followed by

$$OH + CH_3OOH \rightarrow CH_3O_2 + H_2O$$
$$\rightarrow CH_2O + OH + H_2O$$

becomes as important as

$$CH_3O_2 + ClO \rightarrow CH_3O + Cl + O_2$$

According to model calculations;[41] consideration of reaction 1a leads to OH and HO_2 concentrations in the range of (0.5–1) × 10^7 and (1–2) × 10^7 molecules cm^{-3}, respectively in the "ozone hole" region. As a consequence, efficient conversion of HCl to active chlorine can also take place by gas-phase reactions and not only by heterogeneous reactions on NAT and ICE particles allowing rapid catalytic destruction of ozone via the Cl_2O_2 and HOCl cycles. The latter catalytic cycle may, therefore, not be as small as indicated by recent analysis of ozone destruction mechanisms.[42] The potential role of reaction 1 in the photochemistry of the cold stratosphere should, therefore, be thoroughly investigated and stratospheric measurements be made of OH and HO_2 radical concentration distributions.

Registry No. Cl_2, 7782-50-5; CH_4, 74-82-8; Cl_2O, 7791-21-1; O_2, 7782-44-7; ClO, 14989-30-1; CH_3O_2, 690-02-8; ClOO, 17376-09-9; OH, 3352-57-6; H, 12385-13-6; O_3, 10028-15-6.

(41) Brühl, C.; Crutzen, P. J. Quadrennial Ozone Symposium, Göttingen (D), 1988.

(42) Anderson, J. G.; Brune, W. H.; Lloyd, S. A.; Toohey, D. W.; Sander, S. P.; Starr, W. L.; Loewenstein, M.; Podolske, J. R. *J. Geophys. Res.*, in press.

Direct Observation of NF(X) Using Laser-Induced Fluorescence: Kinetics of the NF $^3\Sigma^-$ Ground State

R. F. Heidner III, Henry Helvajian, J. S. Holloway, and J. Brooke Koffend*

Aerophysics Laboratory, The Aerospace Corporation, P.O. Box 92957, Los Angeles, California 90009
(Received: March 1, 1989; In Final Form: May 16, 1989)

The gas-phase kinetics of the NF($X^3\Sigma^-$) ground-state radical have been investigated by direct observation. NF($X^3\Sigma^-$) was produced from the KrF laser photolysis of NF_2 and was directly monitored in the gas-phase by use of laser-induced fluorescence (LIF) via the NF $b^1\Sigma$–$X^3\Sigma^-$ transition. The extremely hot nascent NF($X^3\Sigma^-$) vibrational distribution (T_{vib} = 2350 K) was exploited to investigate vibrational relaxation with CO_2 and SF_6. While CO_2 proved to be inefficient for NF(X) vibrational relaxation ($k_{1-0} = 3.7 \times 10^{-14}$ cm^3/(molecule·s)), SF_6 is a rapid quencher ($k_{1-0} = 1.2 \times 10^{-12}$ cm^3/(molecule·s)). Information on rotational relaxation of NF($X^3\Sigma^-$) was also obtained. The NF ground state is seen to be removed by reaction with NF_2 with a rate coefficient of 2.0×10^{-12} cm^3/(molecules·s). The NF(X) + NF(X) → N_2 + 2F rate coefficient is estimated to be $<5 \times 10^{-12}$ cm^3/(molecule·s), much slower than previously thought.

Introduction

Reactions that involve NF_2 and NF are of interest since many of them produce electronically excited products. In particular, the H_2/NF_2 system[1] serves as a source of metastable NF($a^1\Delta$) which forms the basis for several proposed visible chemical lasers.[2–4] The H_2/NF_2 reaction system has been the subject of several studies where particular attention has been paid to the formation of energetic species.[5–8] The reaction kinetics of the NF($X^3\Sigma^-$) radical and its ultimate fate are critical to a full understanding of this system since it is the principal source of F atoms which propagate the overall chain reaction.

The NF ground state has previously been detected by use of infrared absorption spectroscopy in both the gas phase[9] and in rare gas matrices.[10] Laser-induced fluorescence has also been used to investigate the radiative decay of the NF(a) and NF(b) states in solid argon.[11] There have been several studies[2,5,6] of NF radical reactions with various transient species which include H and N atoms in addition to NF itself. Apart from recent NF(a,b) electronic quenching measurements,[8,12–14] there have been no prior studies on the state-specific kinetics of the NF molecule.

Both NF($a^1\Delta$) and NF($X^3\Sigma^-$) are energetically accessible from the 249-nm photolysis of NF_2 and are produced in 10% and 90% yields, respectively.[8,15] The NF($X^3\Sigma^-$) photofragment is born with a high degree of rotational and vibrational excitation.[16] We have taken advantage of this excited NF($X^3\Sigma^-$) nascent population distribution to perform vibrational and rotational kinetic measurements on the NF ground state. Gas-phase LIF of NF via the b–X transition was employed to directly probe specific rovibrational levels and determine their time behavior.

Experimental Section

A Lumonics 400 Hyperex excimer laser operating with KrF (249 nm) was used as a source of NF($X^3\Sigma^-$) via the photolysis of NF_2, which produces NF($X^3\Sigma^-$) in high yield. The photolysis

(1) (a) Herbelin, J. .; Cohen, N. *Chem. Phys. Lett.* **1973**, *20*, 605. (b) Clyne, M. A. A.; White, I. F. *Chem. Phys. Lett.* **1970**, *6*, 465.
(2) Tennyson, P. H.; Fontijn, A.; Clyne, M. A. A. *Chem. Phys.* **1981**, *62*, 171.
(3) Herbelin, J. M.; Klingberg, R. A. *Int. J. Chem. Kinet.* **1984**, *16*, 849
(4) Coombe, R. D.; Pritt, A. T. *Chem. Phys. Lett.* **1978**, *58*, 606.
(5) Cheah, C. T.; Clyne, M. A. A.; Whitefield, P. D. *J. Chem. Soc., Faraday Trans. 2* **1980**, *76*, 711.
(6) Cheah, C. T.; Clyne, M. A. A. *J. Chem. Soc., Faraday Trans. 2* **1980**, *76*, 1543.
(7) Malins, R. J.; Setser, D. W. *J. Phys. Chem.* **1981**, *85*, 1342.
(8) Koffend, J. B.; Gardner, C. E.; Heidner, R. F. *J. Chem. Phys.* **1985**, *83*, 2904.
(9) Davies, P. B.; Rothwell, W. J. *Proc. R. Soc. London, A* **1983**, *389*, 205.
(10) Milligan, D. E.; Jacox, M. E. *J. Chem. Phys.* **1964**, *40*, 2461.
(11) Becker, A. C.; Schurath, U. *Chem. Phys. Lett.* **1987**, *142*, 313.
(12) Lin, D.; Setser, D. W. *J. Phys. Chem.* **1985**, *89*, 1561.
(13) (a) Cha, H.; Setser, D. W. *J. Phys. Chem.* **1987**, *91*, 3658. (b) Cha, H.; Setser, D. W. *J. Phys. Chem.* **1989**, *93*, 235.
(14) Quinones, E.; Habdas, J.; Setser, D. W. *J. Phys. Chem.* **1987**, *91*, 5155.
(15) Heidner, R. F.; Helvajian, H.; Koffend, J. B. *J. Chem. Phys.* **1987**, *87*, 1520.
(16) Heidner, R. F.; Helvajian, H.; Holloway, J. S.; Koffend, J. B. To be published.

0022-3654/89/2093-7813$01.50/0